



Functional evaluation of tryptophans in glycolipid binding and membrane interaction by HET-C2, a fungal glycolipid transfer protein

Roopa Kenoth^a, Xianqiong Zou^{b,1}, Dhirendra K. Simanshu^{c,2}, Helen M. Pike^b, Lucy Malinina^b, Dinshaw J. Patel^c, Rhoderick E. Brown^b, Ravi Kanth Kamlekar^{a,*,3}

^a Dept. of Chemistry School of Advanced Sciences, VIT, Vellore, Tamil Nadu 632014, India

^b The Hormel Institute, University of Minnesota, 801 16th Ave NE, Austin, MN 55912, USA

^c Memorial Sloan-Kettering Cancer Ctr, New York, NY, USA

ARTICLE INFO

Keywords:

Trp point mutation
Fluorescence
HET-C2
GLTP
Membrane binding
GLTP-fold
Glycosphingolipid transfer

ABSTRACT

HET-C2 is a fungal glycolipid transfer protein (GLTP) that uses an evolutionarily-modified GLTP-fold to achieve more focused transfer specificity for simple neutral glycosphingolipids than mammalian GLTPs. Only one of HET-C2's two Trp residues is topologically identical to the three Trp residues of mammalian GLTP. Here, we provide the first assessment of the functional roles of HET-C2 Trp residues in glycolipid binding and membrane interaction. Point mutants HET-C2^{W208F}, HET-C2^{W208A} and HET-C2^{F149Y} all retained > 90% activity and 80–90% intrinsic Trp fluorescence intensity; whereas HET-C2^{F149A} transfer activity decreased to ~55% but displayed ~120% intrinsic Trp emission intensity. Thus, neither W208 nor F149 is absolutely essential for activity and most Trp emission intensity (~85–90%) originates from Trp109. This conclusion was supported by HET-C2^{W109Y/F149Y} which displayed ~8% intrinsic Trp intensity and was nearly inactive. Incubation of the HET-C2 mutants with 1-palmitoyl-2-oleoyl-phosphatidylcholine vesicles containing different monoglycosylceramides or presented by lipid ethanol-injection decreased Trp fluorescence intensity and blue-shifted the Trp λ_{\max} by differing amounts compared to wtHET-C2. With HET-C2 mutants for Trp208, the emission intensity decreases (~30–40%) and λ_{\max} blue-shifts (~12 nm) were more dramatic than for wtHET-C2 or F149 mutants and closely resembled human GLTP. When Trp109 was mutated, the glycolipid induced changes in HET-C2 emission intensity and λ_{\max} blue-shift were nearly nonexistent. Our findings indicate that the HET-C2 Trp λ_{\max} blue-shift is diagnostic for glycolipid binding; whereas the emission intensity decrease reflects higher environmental polarity encountered upon nonspecific interaction with phosphocholine headgroups comprising the membrane interface and specific interaction with the hydrated glycolipid sugar.

In filamentous fungi such as *Podospora anserina*, cell-cell recognition associated with heterokaryon fusion and vegetative incompatibility is regulated by *het* genes [1]; [2]. The heterokaryon compatibility gene, *het-c2*, encodes HET-C2, a protein with similar conformational architecture to human glycolipid transfer protein, i.e. GLTP-fold [3]; [4]; [5]; [6]; [7]; [8]. HET-C2 uses its all α -helical, two-layer 'sandwich' topology to bind and transfer single glycosphingolipid (GSL) molecules between membranes in vitro [7]; [8]; [9]; [10]. To acquire and deliver glycolipids, HET-C2 must interact transiently and reversibly with membranes. Thus, HET-C2 possesses the defining features of peripheral

amphitropic membrane proteins, which have affinity for both aqueous and nonpolar environments but require neither post-translational modifications nor anchor proteins for reversible interaction with membranes [3]; [5]; [8].

Currently, there is much interest in defining the specific and non-specific ways that membrane lipid composition can target amphitropic proteins, such as HET-C2 and human GLTP, to select sites in cells. One approach to track protein interaction with membranes relies on the environmentally responsive fluorescence of tryptophan (Trp) to avoid disturbances introduced by extrinsic labels. Human GLTP contains

Abbreviations: GLTP, glycolipid transfer protein; GSL, glycosphingolipid; MonoGlycCer, monoglycosylceramide; GalCer, galactosylceramide; GlcCer, glucosylceramide; POPC, 1-palmitoyl-2-oleoyl-*sn*-glycero-3-phosphocholine; SUVs, small unilamellar vesicles

* Corresponding author: Dept. of Chemistry, School of Advance Sciences, VIT, Vellore 632014, India.

E-mail address: ravikanth.k@vit.ac.in (R.K. Kamlekar).

¹ Present address: College of Biotechnology, Guilin Medical University, Guilin 541100, Guangxi, P.R. China.

² Present address: Frederick National Laboratory of National Cancer Institute, Frederick, MD, USA.

³ <http://vit.ac.in/academics/schools/sas/faculty>.

<https://doi.org/10.1016/j.bbamem.2018.01.001>

Received 5 November 2017; Received in revised form 16 December 2017; Accepted 1 January 2018

Available online 03 January 2018

0005-2736/ © 2018 Elsevier B.V. All rights reserved.

three Trp residues [11]. A complicating feature of human GLTP Trp fluorescence is the dramatically different contribution of each Trp to the total emission, with Trp96, Trp142, and Trp85 accounting for 70–75%, 15–20%, and 5–10% of the signal [12]. The situation is made more complex by the so-called ‘signature’ Trp fluorescence response triggered in GLTP upon interaction with membranes containing glycolipid [11]; [12]; [13]; [14]. The resulting drop in fluorescence intensity (~40%) and 12–13 nm blue shift in the emission wavelength maximum (λ_{\max}) correlates with glycolipid binding via stacking of the initial ceramide-linked sugar headgroup over Trp96. This positioning of Trp96 in the GSL headgroup recognition center was initially observed by X-ray diffraction [3]; [4]; [5]; [6]. Point mutation to either Phe or Ala supported the importance of Trp96 for proper function of the glycolipid headgroup recognition center [3]. Double mutation of Trp to Phe (homo) in various combinations verified the importance of Trp96 but provided limited insights into the functionality of other Trp residues [13]. A hetero double mutation strategy involving replacement of Trp with Phe and Tyr enabled adequate protein viability to dissect the various functional roles played by each of GLTP's three Trps including the participation of Trp142 in the initial membrane docking event [12]. The importance of Trp142 to GLTP functionality was made dramatically clear by the severely impaired membrane partitioning and loss of glycolipid transfer induced by Trp142-to-Ala point mutation [15]. Yet, mapping of the complete GLTP-fold membrane interaction site remains defined mostly by modeling [5]; [8]; [12]; [16]; [17]; [18]; [19].

The HET-C2 GLTP-fold contains only two Trp residues. Trp208 forms the C-terminus in the HET-C2 GLTP-fold and resides on the protein surface as determined by X-ray diffraction (1.9 Å) [8]. The location and accessibility of Trp208 differ from GLTP Trp85 and Trp142, the latter which participates in the initial events of membrane docking [12]; [15]; [20]. In contrast, Trp109 is structurally homologous with Trp96 in human GLTP/glycolipid complexes suggesting a stacking function that helps orient the ceramide-linked sugar for hydrogen bonding with conserved Asp, Asn, Lys, and His in the glycolipid headgroup recognition center [8]. In the present study, we provide the first evaluation of Trp functionality in the fungal GLTP-fold using point mutation approaches. Our study provides evidence for: i) Trp109 playing a key role in the binding of glycolipid as well as enhancing HET-C2 partitioning to the POPC membranes; ii) Phe149, which replaces Trp in some other GLTP orthologs, regulating membrane interaction needed for efficient and rapid transfer of simple uncharged GSLs; iii) W208 playing a minimal role regulating the transfer activity of monoglycosylceramides (MonoGlycCer) and membrane partitioning of HET-C2.

1. Experimental procedures

1.1. Expression and purification of wild type HET-C2 and mutants of HET-C2

The *P. anserina* ORF encoding HET-C2 (NCBI GenBank # U05236) was subcloned into pET-30 Xa/LIC (Novagen) by Ligation Independent Cloning [8]. HET-C2 mutants (W208F, W208A, F149Y, F149A, H101A, W109Y and W109Y-F149Y) were produced by QuikChange mutagenesis (Stratagene, La Jolla, CA) and confirmed by sequencing. Mutant and wild-type constructs (pET-30 Xa/LIC; Novagen) were transformed into BL21 cells, grown in Luria-Bertani medium at 37 °C, induced with 0.1 mM IPTG, and then grown 16–20 h at 15 °C. Soluble protein from lysate was isolated by Ni-NTA affinity chromatography. Final purification was accomplished by FPLC SEC using a HiLoad 16/60 Superdex-75 prep grade column (Amersham). Protein purity was verified by SDS-PAGE.

1.2. Glycolipid transfer of HET-C2

Radiolabeled glycolipid transfer between vesicles was measured at

37 °C by incubating with HET-C2 (0.2–0.5 µg) with donor vesicles [1-palmitoyl-2-oleoyl phosphatidylcholine (POPC) + 10 mol% dipalmitoyl phosphatidic acid] containing [³H]-GalCer (2 mol%), a trace of nontransferable [¹⁴C]-tripalmitin and ten-fold excess of POPC acceptor vesicles. After recovery of the acceptor vesicles by passage of the mixture over DEAE-Sepharose minicolumns, glycolipid transfer was quantified by liquid scintillation counting [21].

1.3. Preparation of vesicles

Lipid mixtures, dissolved in dichloromethane, were dried under a gentle stream of nitrogen in a glass test tube. Final traces of solvent were removed by vacuum desiccation for > 3 h. The dried lipid film was hydrated by vortexing for 5 min with 10 mM phosphate buffered saline (pH 7.4). Small unilamellar vesicles (SUVs) were prepared by intermittent probe sonication of the lipid suspension for about 30–45 min at room temperature. Residual multilamellar vesicles and titanium probe particles were removed by centrifugation at 100,000g for 90 min. Analysis by size exclusion chromatography confirmed average diameters of ~25–30 nm for SUVs [22].

1.4. Fluorescence measurements

Trp fluorescence was measured at 25 °C from 310 to 420 nm with a SPEX FluoroMax steady state fluorimeter (Horiba Scientific) using excitation and emission band passes of 5 nm while exciting at 295 nm. Protein concentration was kept at $A_{295} < 0.1$ to avoid inner filter effects [14]. For membrane interaction studies, the Trp emission signals of wtHET-C2 and mutants (1 µM) were measured before and after addition of increasing amounts of POPC vesicles lacking or containing glycolipid (20 mol%). HET-C2 binding of glycolipid also was assessed by titration-microinjection of glycolipids (or other lipids) dissolved in ethanol [14]. Measurements were performed under constant stirring adding small aliquots (1 µl) of GSL, dissolved in ethanol (0.1 mM), to protein (1 µM; 2.5 ml).

1.4.1. Binding/partitioning coefficient analyses

Because the Trp emission peak undergoes a dramatic λ_{\max} blue-shift (355 to ~348 nm) upon glycolipid binding, intensities at 353 nm were used to evaluate binding isotherms to avoid problems discussed by [23]. The fraction of binding sites (α) occupied by glycolipids was calculated by Eq. (1):

$$\alpha = (F - F_0) / F_{\max} \quad (1)$$

where F_0 and F are the Trp emission intensities of GLTP in the absence and presence of glycolipid, respectively, and F_{\max} is the emission intensity of the fully liganded GLTP, i.e. at excess glycolipid [24]; [25]. F_{\max} was determined by plotting $1/(F - F_0)$ vs. $1/L$ and extrapolating $1/L = 0$, where L equals the total glycolipid concentration. ΔF_m (maximum fluorescence change when the protein is completely saturated with glycolipid) was determined by plotting $1/L$ (glycolipid concentration) and $1/\Delta F$ (decrease in fluorescence intensity). The bound glycolipid concentration was calculated using the relationship:

$$[\text{Bound Lipid}] = -\text{protein concentration} \times \Delta F / \Delta F_m \quad (2)$$

The free lipid concentration was calculated as:

$$[\text{Free lipid}] = [\text{Total lipid}] - [\text{Bound lipid}] \quad (3)$$

K_d values shown in Table 3 were determined by nonlinear least-squares (NLLSQ) fitting of bound lipid vs. free lipid. NLLSQ and regression analyses and data simulations were performed using OriginPro 7.0 software (MicroCal, Inc., Northampton, MA) and Prism 5 (GraphPad Software, Inc. La Jolla, CA) to avoid biases associated with linear transformations, i.e. Scatchard analysis. Our previous mass spectroscopy analyses of HET-C2:glycolipid complexes indicate binding of one glycolipid per protein [8].

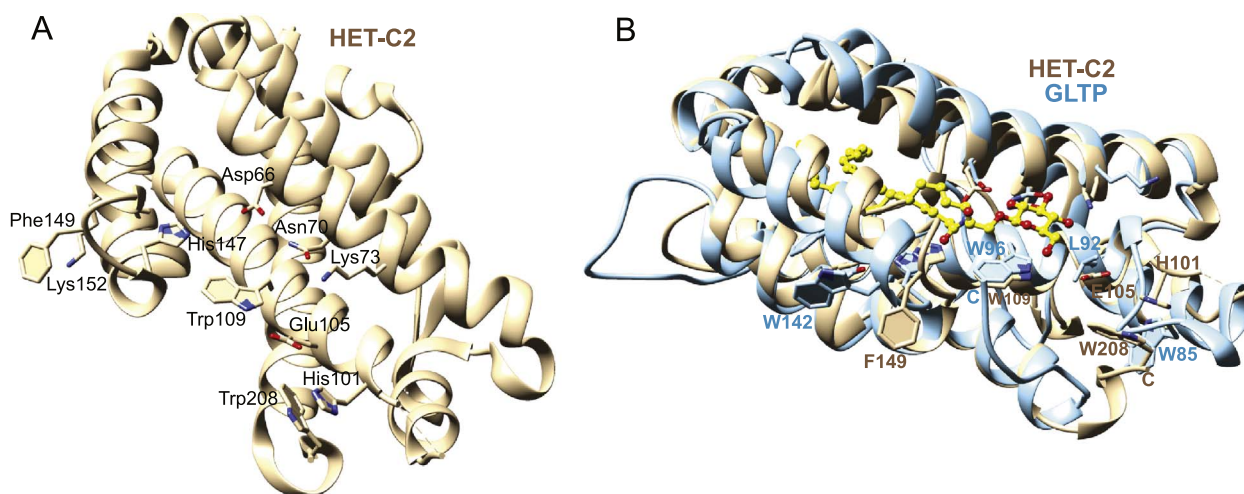


Fig. 1. HET-C2 Trp locations compared to GLTP. A) The locations of Trp¹⁰⁹, Trp²⁰⁸ and Phe¹⁴⁹ in the HET-C2 GLTP-fold are shown along with interacting residues of the sugar head group recognition site (Asp⁶⁶, Asn⁷⁰, Glu¹⁰⁵, Lys⁷³, His¹⁴⁷). The HET-C2 GLTP-fold (PDB 3kv0) was determined previously [8] by X-ray diffraction (1.9 Å). B) Superpositioning of the X-ray structures of HET-C2 (beige; PDB 3kv0) and human GLTP (cyan; PDB 3s0k) complexed with GlcCer (yellow).

Fluorescence titration curves by the ethanol injection method were analyzed according to:

$$\epsilon - 1 = (\epsilon_b - 1) - K_d(\epsilon - 1)/m \quad (4)$$

where K_d is the dissociation constant of lipid-protein complex, m is lipid concentration and n is number of lipid binding sites [26]; [27]. The quantity ϵ is the relative value of the spectral parameter (peak emission wavelength, λ_{\max} , or intensity, I) accompanying lipid binding to HET-C2 at lipid concentration m . Thus, ϵ can represent either I/I_0 or $(\lambda_{\max})_0/\lambda_{\max}$ where the 0 subscript equals values in the absence of lipid. The parameter ϵ_b represents spectral properties of the protein-lipid complex. According to Eq. (4), the slope of $\epsilon-1$ versus $(\epsilon-1)/m$ yields K_d/n , the reciprocal of the protein/lipid association constant.

2. Results

Superpositioning of previously determined X-ray structures for apo-HET-C2 (PDB 3KV0; 1.9 Å) and human apo-GLTP (PDB 3RWV; 1.5 Å) or apo-HET-C2 and human GLTP complexed with N-oleoyl glucosylceramide (GlcCer) (PDB S0K; 1.4 Å) illustrates their global conformational similarities as well as the locations of their Trp residues [8]; [28]. Fig. 1 shows the nearly identical positioning of HET-C2 W109 and GLTP W96 within the glycolipid sugar headgroup recognition center. By contrast, the C-terminal Trp208 of HET-C2 resides on the surface, but is not buried like GLTP Trp85 and is located differently than Trp142 (helix-6 surface). The Trp208 indole ring undergoes a stacking interaction with the imidazole ring of His101 in the $\alpha 3$ - $\alpha 4$ loop. This positioning suggests a possible role in membrane interaction and/or as a ‘gatekeeper’ for glycolipid binding. Also noteworthy is the similar location of HET-C2 Phe149 on α -helix 6 compared to GLTP Trp142. In this regard, Phe is somewhat unusual because Trp occurs at this position in most eukaryotic GLTP orthologs [6]; [29]; [30]. To evaluate the functional roles of the HET-C2 residues, several point mutants were generated including HET-C2^{W208A}, HET-C2^{W208F}, HET-C2^{F149Y}, HET-C2^{F149A} and HET-C2^{W109Y/F149Y}. Self-aggregation during expression and purification prevented successful production of HET-C2^{W109Y} and HET-C2^{H101A} as soluble monomers.

2.1. Transfer activity of HET-C2 point mutants

The transfer rates of radiolabeled galactosylceramide (GalCer) between membrane vesicles by the HET-C2 mutants and wtHET-C2 were

determined as outlined in the Methods [10]; [21] and are shown in Fig. 2A. Compared to wtHET-C2, the W208F, W208A and F149Y point mutants retained > 88% activity; whereas the transfer activity of HET-C2^{F149A} decreased to ~55% (Table 1). The aromatic ring side-chain of Tyr in HET-C2^{F149Y} did a better job of maintaining HET-C2 transfer activity compared to nonaromatic Ala in HET-C2^{F149A}. The findings indicate that F149 is more important than W208 for HET-C2 to maintain GlcCer intervesicular transfer. Notably, the double mutant, HET-C2^{W109Y/F149Y} left the protein nearly inactive. Considering the minimal effect of F149Y mutation, the data support the major role of Trp109 in HET-C2 transfer activity.

2.2. Trp fluorescence of HET-C2 mutants

Determination of the Trp emission profiles of the HET-C2 mutants was performed (Fig. 2B). The peak Trp emission intensities of HET-C2^{W208F} and HET-C2^{W208A} were ~90% and 80%, respectively, compared to wtHET-C2; whereas the HET-C2^{F149A} and HET-C2^{F149Y} emission intensities were ~120% and 80%, respectively. The drop in Trp emission intensity by HET-C2^{F149Y} likely reflects quenching by Tyr of nearby Trp109 [31]. In contrast, HET-C2^{W109Y/F149Y} emitted at only ~8% of the intensity of wtHET-C2. The results imply that ~80–85% of the total Trp emission intensity in wtHET-C2 comes from Trp109, whereas, only 15–20% originates from W208. Possible reasons for the minor contribution by W208 to the overall Trp emission could be quenching associated via its stacking interaction with H101 as well as exposure to the highly polar environment on the surface of HET-C2.

2.3. HET-C2 fluorescence changes induced by membranes containing or lacking GSLs

In human GLTP, glycolipid binding induces changes in Trp emission fluorescence, i.e. ~35–40% intensity decrease and ~12 nm blue shift in λ_{\max} , that are almost entirely attributable to stacking of the ceramide-linked sugar over Trp96 of the sugar headgroup recognition site [14]. Incubation of wtHET-C2 not previously exposed to glycolipid with membrane vesicles containing glycolipid also induces substantial decreases (25–30%) in Trp emission intensity and blue-shifts in emission λ_{\max} (6–7 nm), albeit diminished in magnitude compared to human GLTP [8]. With all HET-C2 mutants except HET-C2^{W109Y/F149Y} (Fig. 3), the Trp λ_{\max} blue-shift and intensity changes observed upon the

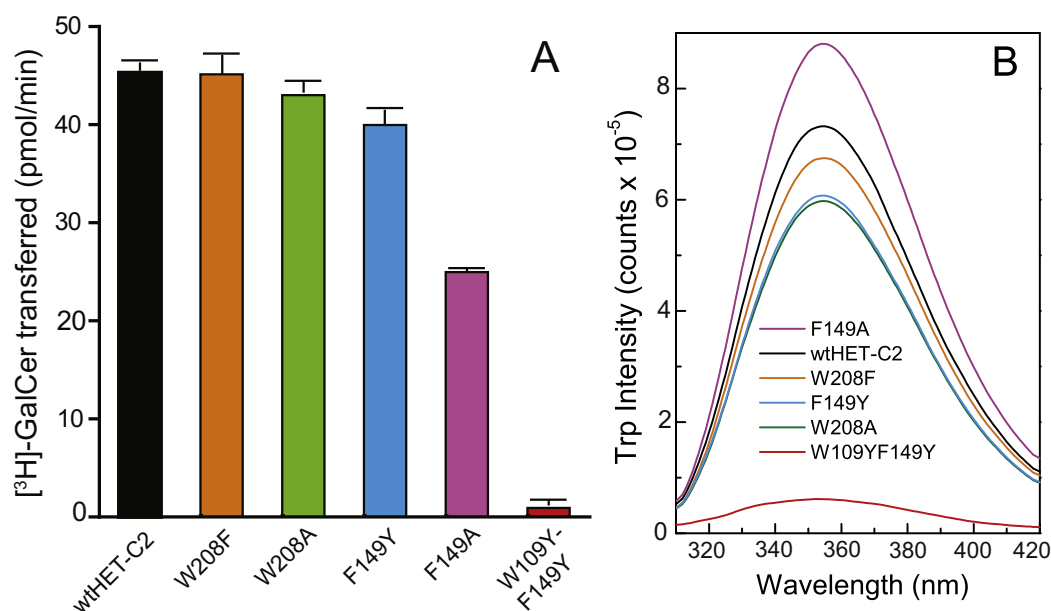


Fig. 2. Glycolipid transfer activities and Trp fluorescence of HET-C2 mutants. A) Glycolipid transfer rates of wtHET-C2 and HET-C2 mutants. Radiolabeled glycolipid intervesicular transfer was measured at 37 °C by incubating protein (0.5 µg) with POPC donor vesicles containing [³H]-GalCer (2 mol%) and 10 mol% dipalmitoyl phosphatidic acid and POPC acceptor vesicles (10 × excess). See the [Exptl. Procedures](#) for more details. B) Trp emission spectra (top to bottom) for HET-C2^{F149A} (magenta), wtHET-C2 (black), HET-C2^{W208F} (orange), HET-C2^{F149Y} (cyan), HET-C2^{W208A} (green) and HET-C2^{W109Y-F149Y} (red) were obtained in phosphate-buffered saline at pH 7.4 by exciting at 295 nm at 25 °C. Additional details are provided in the [Exptl. Procedures](#).

Table 1
Glycolipid transfer activity of mutants compared to wtHET-C2.

Protein	% Activity
wtHET-C2	100 ± 1.4
HET-C2 ^{W208F}	99.6 ± 3.6
HET-C2 ^{W208A}	94.9 ± 1.9
HET-C2 ^{F149Y}	88.2 ± 2.2
HET-C2 ^{F149A}	55.1 ± 3.0
HET-C2 ^{W109Y-F149Y}	2.03 ± 0.04

stepwise addition of vesicles containing glycolipid were increased in magnitude compared to wtHET-C2 and were very similar to those of human GLTP (Table 2). For instance, HET-C2^{W208F} showed a maximum λ_{\max} blue-shift of ~12 nm and a ~30–40% reduction in emission intensity. Other HET-C2 mutants also displayed Trp λ_{\max} blue shifts of ~9–12 nm. With the HET-C2 mutants, the emission intensity decreases also were larger in magnitude than for wtHET-C2 with HET-C2^{F149A} displaying the most emission quenching (~40%). In the case of weakly emitting HET-C2^{W109Y-F149Y}, the emission changes were more complex and much less dramatic due to the absence of the strongly emitting W109. An initial intensity increase was followed by a small reduction in intensity and there was no accompanying λ_{\max} blue shift. The implication is that Trp109 has major role in the binding and partitioning of lipids to HET-C2. When the sugar headgroup of MonoGlycCer was changed from glucose to galactose, the dramatic λ_{\max} blue shifts and intensity reductions persisted but displayed subtle differences (Table 2). For instance, slightly larger λ_{\max} blue-shifts were observed for the F149 mutants and wtHET-C2 when the POPC vesicles contained GlcCer rather than GalCer. The partitioning isotherms for the various HET-C2 mutants to POPC vesicles either containing or lacking GlcCer or GalCer are shown in Fig. 4. Estimates of the resulting K_d values for the various HET-C2 mutants are summarized in Table 3. Generally, the K_d values were higher compared to that of wtHET-C2. The K_d value for protein partitioning to POPC membranes was estimated to be ~4–5 µM, a value

that remained largely unaffected for all mutants except for HET-C2^{W109Y-F149Y}. Estimates of the K_d value for this mutant were deemed unreliable because the changes were small. Here again, the implication is that Trp109 has major role in the binding and partitioning of lipids to HET-C2.

2.4. Presentation of lipids to HET-C2 via ethanol-microinjection

Previously, we found that microinjection of small lipid aliquots dissolved in ethanol provides a way to load the glycolipid binding site of GLTP or HET-C2 while minimizing the accumulation of excess membrane interface in solution, thus providing a means to distinguish emission changes induced by glycolipid binding from changes produced by nonspecific partitioning to membrane interface [8]; [14]. Fig. S1 shows the Trp emission response of HET-C2 mutants, titrated with lipid using the EtOH-microinjection approach. With each successive injection of glycolipid, the HET-C2 Trp emission λ_{\max} became progressively more blue-shifted and the fluorescence intensity systematically diminished (20–30%) in similar fashion as with POPC vesicles containing glycolipid. Yet, the magnitude of the intensity reduction was diminished compared to that of SUVs with glycolipid (Table S1). Also, the λ_{\max} blue-shift was diminished compared to HET-C2^{F149Y} and HET-C2^{F149A}. These mutants displayed similar fluorescence quenching when injected with glycolipid-free POPC, which forms liposomes that interact non-specifically. In the case of weakly emitting HET-C2^{W109Y-F149Y}, the quenching was nominal presumably reflecting the absence of the strongly emitting W109.

3. Discussion

Our point mutational data support Trp109 functioning as a stacking plate that orients the initial ceramide-linked sugar to facilitate formation of the hydrogen bond network with Asp66, Asn70, Lys73, and Glu105 [6]; [7]; [8]. Unexpectedly, we found no evidence for Trp208 involvement in membrane interaction despite its proximity to the GSL

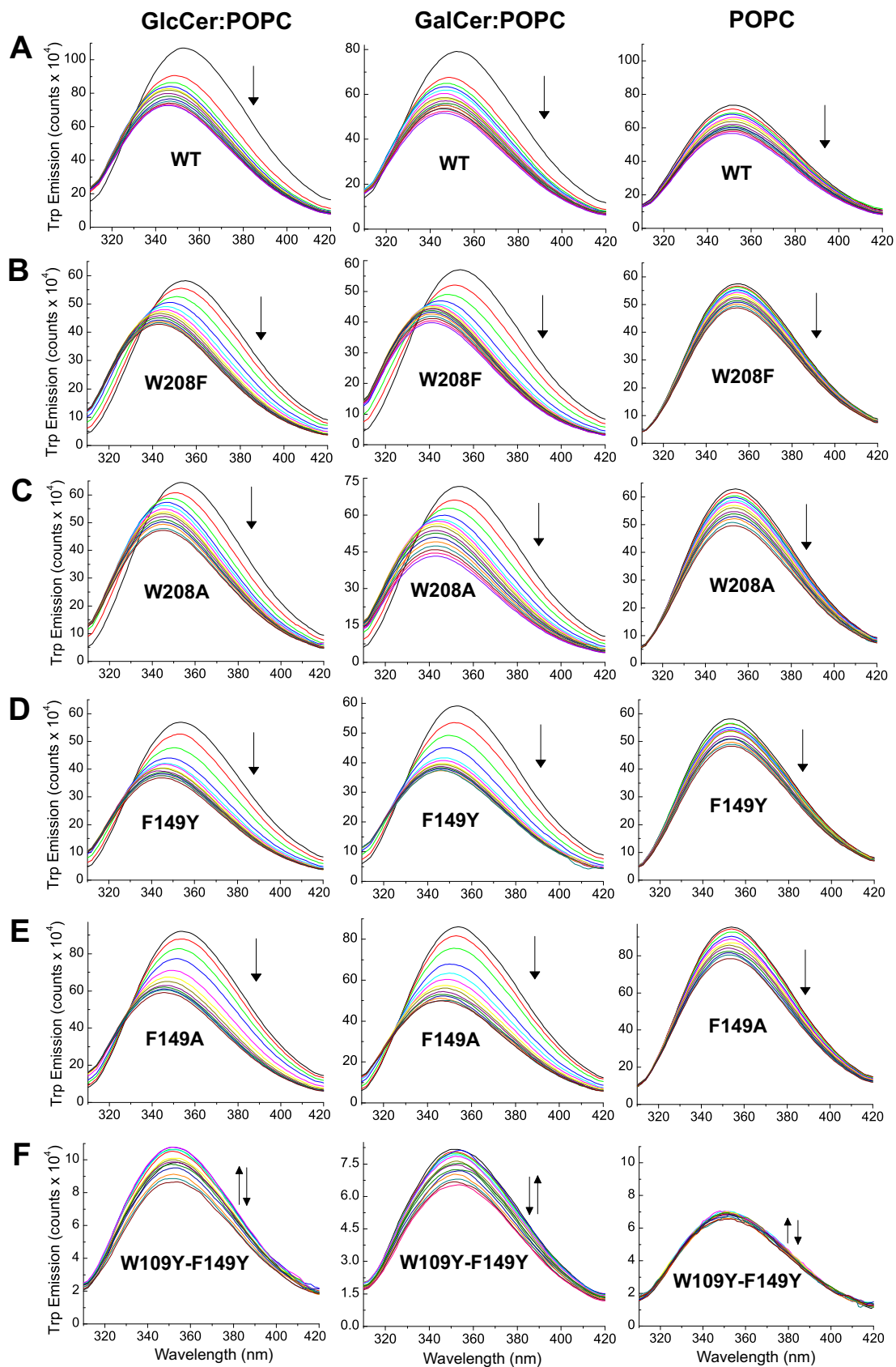


Fig. 3. Fluorescence response of wtHET-C2 and mutants to titrations with POPC SUVs containing or lacking either GlcCer or GalCer (20 mol%). Vesicles were introduced in stepwise fashion with proteins (1 μ M) and incubated for 5 min between injections as detailed in [8]. Control injections enabled correction for dilution effects. Emission spectra were measured as described in the [Exptl. Procedures](#).

Table 2

Trp emission changes in HET-C2 mutants induced by interaction with membranes containing or lacking glycolipid. Values for wtGLTP and GLTP^{W96F} are from [14] and for FAPP2-GLTPH are from [19].

Protein	POPC (SUV)			POPC:GlcCer (8:2) SUV			POPC:GalCer (8:2) SUV		
	Intensity (% change)	Blue shift	Red shift	Intensity (% change)	Blue shift	Red shift	Intensity (% change)	Blue shift	Red shift
wtHET-C2	17↓	1		26↓	7		29↓	6	
HET-C2 ^{W208F}	18↓	1		28↓	12		30↓	12	
HET-C2 ^{W208A}	19↓	2		25↓	9		40↓	11	
HET-C2 ^{F149Y}	20↓	–		37↓	10		39↓	8	
HET-C2 ^{F149A}	21↓	1,2		38↓	8		42↓	7	
HET-C2 ^{W109Y-F149Y}							20↓		2
wtGLTP		1					40↓	12	
GLTP ^{W96F}							4–5↓		2–3
FAPP2-GLTPH	22↓	1					30↓	14	

headgroup recognition center, accessibility, and unique C-terminal location. Rather, the data indicate that Phe149 plays the more important role in regulating the transient membrane interaction needed for efficient and rapid transfer of simple uncharged GSLs by HET-C2.

3.1. Phe149 function

Orientation of Proteins in Membranes (OPM) modeling and surface hydrophobicity analyses had predicted direct involvement of Phe149 in HET-C2 docking to membranes [8]. Phe149 along with Leu150, Pro153, Ile154, and Ala157 of helix 6 and Ile58 of the adjacent 1–2 loop form a hydrophobic patch that promotes membrane docking. Compared to mutation to Ala, replacement of the large nonpolar Phe149 with the somewhat more polar Tyr only slightly increases the membrane dissociation constant, consistent with minimal effect on transfer activity and λ_{\max} blue-shift. Yet, F149 mutation to Tyr also preserves an aromatic side-chain which may facilitate high transfer activity by undergoing cation- π interaction with K152.

With HET-C2^{F149A}, the lower transfer activity is surprising given the high Trp emission intensity and λ_{\max} blue-shift (\geq wtHET-C2) that indicate no diminished docking by HET-C2^{F149A} to membranes containing glycolipid, a conclusion supported by the partitioning isotherms. To reconcile the data, we speculate that when F149 is mutated to Ala, the F149/K152 cation- π interaction is disrupted, triggering local conformational changes that disturb HET-C2 residues involved in the gating action needed for glycolipid uptake. As illustrated in Fig. S3, Phe155 in helix- α 6 of apoHET-C2 is positioned similarly to Phe148 in helix- α 6 of apo-GLTP in a ‘closed gate’ conformation that obstructs glycolipid entry into the hydrophobic pocket [3]; [28]. After glycolipid uptake, the benzyl side chain of Phe148 shifts to an ‘open gate’ conformation to enable glycolipid aliphatic chain entry into the hydrophobic pocket during membrane interaction [3]; [4]; [5]; [28]. We speculate a similar ‘gate open’ conformation for Phe155 of HET-C2 enables glycolipid uptake. In GLTP, the ‘gate open’ conformation of Phe148 is stabilized by π - π stacking from beneath by Tyr132 in helix- α 5. We propose that the similarly positioned Tyr139 in HET-C2 plays the same role of stabilizing the ‘gate open’ conformation of HET-C2 Phe155. In GLTP, Tyr132 also stabilizes the orientation of His140 that interacts with the glycolipid amide linkage to properly orient the sphingoid and acyl chains of ceramide during GSL uptake. Tyr139 of HET-C2 is expected to interact similarly with His147. Thus, mutations that affect Tyr132 positioning in GLTP and Tyr139 in HET-C2 are expected to significantly impact transfer protein function even when protein partitioning to the membrane is marginally affected. We propose that when F149 is mutated to Ala, the broken cation- π interaction between F149 and K152 affects membrane interaction in ways that

alter the critically important conformation of Tyr139. Testing of these ideas will require future structural evaluation of the positioning of Phe155, Tyr139, and His147 in the apo and holo forms of HET-C2^{F149A} and HET-C2^{F149Y}.

3.2. Trp208 function

The π - π stacking of W208 and H101 in apoHET-C2 led us to previously propose a role for W208 in protein folding and stabilization in solution [9] analogous to W85 stabilization in GLTP [12]. However, the current mutational analyses do not support an essential need for W208 in HET-C2 to maintain stability and function. Indeed, both MonoGlycCer transfer activity and Trp emission intensity are minimally affected by W208F and W208A point mutants suggesting a nonessential role for W208. The moderately lowered Trp emission intensity levels reflect the absence of W208 which contributes only ~15% to the total Trp emission signal in wtHET-C2. The signature λ_{\max} blue-shift and fluorescent intensity changes observed during the incubation of W208F and W208A mutants with glycolipid containing membranes are actually more pronounced than those of wtHET-C2 and very similar to those of GLTP and FAPP2 [14]; [19]. This could indicate a favorable topological change of the surface region adjacent to the HET-C2 sugar recognition center. In HET-C2, Glu105 is located similarly to Leu92 in GLTP. Glu105 forms a water-bridged hydrogen bond with H101 that helps orient the imidazole ring for stacking against indole ring of Trp208 [9]. This interaction system, that shapes the region adjacent to the sugar headgroup recognition center of HET-C2, could be perturbed by mutation of W208 to Ala (simple and nonpolar) and to a lesser extent, by W208 mutation to Phe (aromatic and nonpolar). The expected consequence, especially for HET-C2^{W208A}, would be slight alteration of the pit-like morphology for the HET-C2 sugar head group recognition center that so ideally engages with simple uncharged sugar head groups [6]. Although the mutational changes only marginally impact the transfer activity of MonoGlycCer, the proposed gate-keeper role for Trp208 could become more evident with complex GSL ligands, thus explaining the focused transfer specificity of HET-C2 for simple neutral GSLs compared to mammalian GLTPs.

Finally, our previous structural modeling indicated that Glu105 can form two H-bonds with glucose versus one H-bond with galactose [8]. Interestingly, wtHET-C2, HET-C2^{F149Y}, and HET-C2^{F149A} all display a slightly greater λ_{\max} blue shift upon mixing with POPC vesicles containing GlcCer compared to GalCer but Trp208 point mutants do not. It is tempting to speculate that this difference reflects a slight Glu105-driven preference of HET-C2 for GlcCer over GalCer an idea also supported by the K_d values of the various mutants (Table 3).

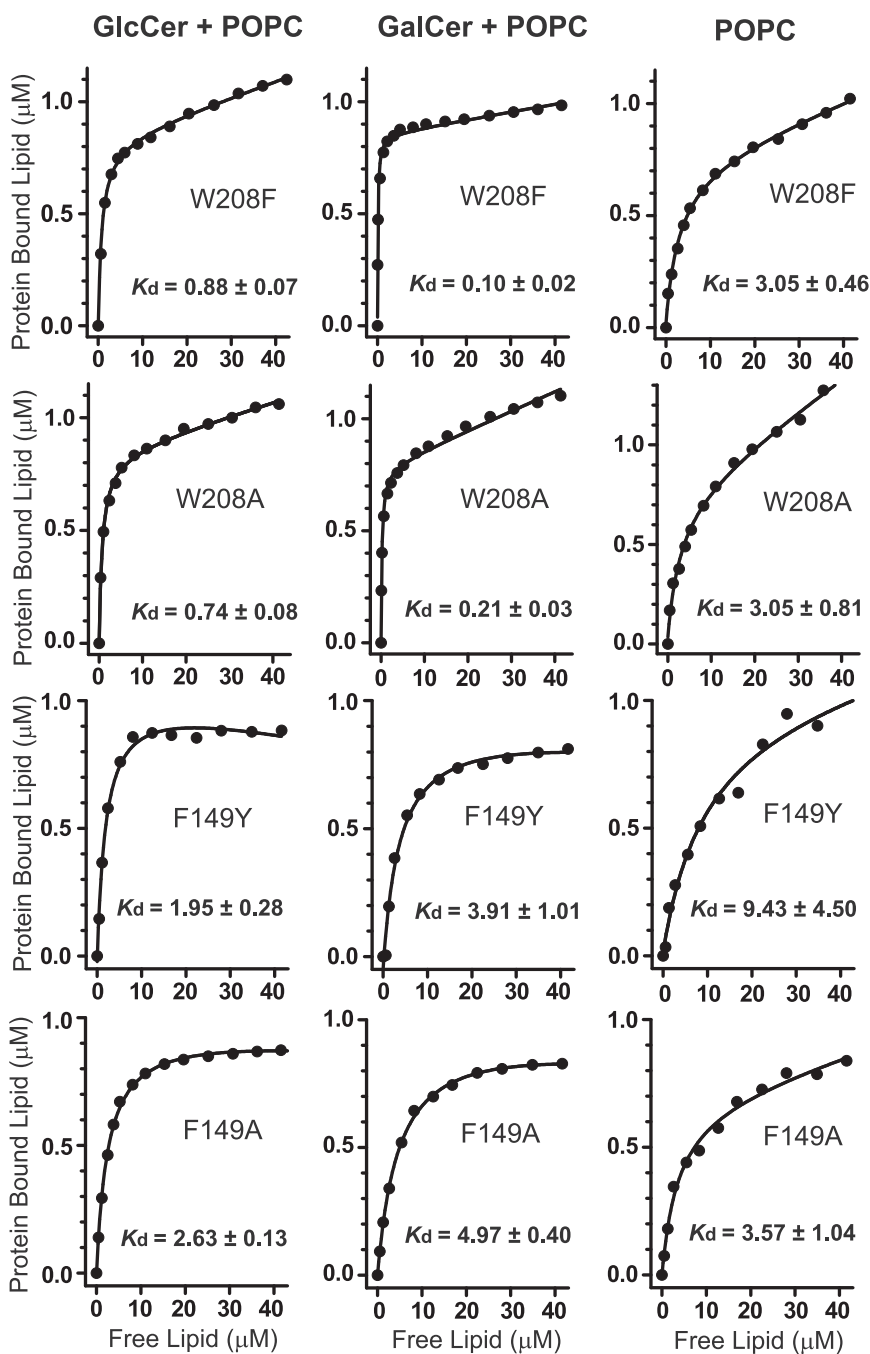


Fig. 4. Partitioning isotherms for the various HET-C2 mutants to POPC vesicles containing or lacking either GlcCer or GalCer (20 mol%). Analyses of the partitioning isotherms were performed from the vesicle titration data (shown in Fig. 3) as described in the Exptl. Procedures.

Table 3

Partitioning constant (K_d) values for various mutants involving POPC vesicles containing or lacking MonoGlycCer. Partitioning constants (K_d) were determined from the fluorescence intensity changes as described in the Exptl. Proc. *Values for wtHET-C2 determined previously by Kenoth et al. [8] were comparable to newly calculated values shown in Fig. S2.

	K_d (μM)		
	GalCer	GlcCer	POPC
wtHET-C2	0.11 \pm 0.1*	0.13 \pm 0.1*	5.26 \pm 1.39*
W208A	0.21 \pm 0.03	0.74 \pm 0.08	3.05 \pm 0.81
W208F	0.10 \pm 0.02	0.88 \pm 0.07	3.05 \pm 0.46
F149A	4.97 \pm 0.40	2.63 \pm 0.13	3.57 \pm 1.04
F149Y	3.79 \pm 1.01	1.95 \pm 0.28	9.43 \pm 4.50

In summary, the functional data presented here indicate that Trp109 plays a significant role in the binding of glycolipid and enhancement of HET-C2 partitioning to PC membranes. In contrast, role of Trp208 appears to be much less essential for maintaining MonoGlycCer intermembrane transfer. Phe149 in helix-6 appears to play an important analogous role as Trp142 in GLTP by promoting membrane interaction that optimizes the transfer process.

5. Transparency document

The <http://dx.doi.org/10.1016/j.bbamem.2018.01.001> associated with this article can be found, in online version.

Acknowledgments

We are grateful for support from Dept. of Science and Technology, Science and Engineering Research Board (SERB), Govt. of India to Ravi Kanth Kamlekar (YSS/2014/000021) and to Roopa Kenoth (YSS/2015/000783) as well as support by NIH/NIGMS-GM45928 (to REB), NIH/NCI-CA121493 (to DJP & REB), NIH/NHLBI-HL125353 (to DJP & REB) and the Hormel Foundation. We thank VIT for research facilities and infrastructure.

Appendix A. Supplementary data

Supplementary data to this article can be found online at <https://doi.org/10.1016/j.bbamem.2018.01.001>.

References

- [1] N.L. Glass, I. Kaneko, Fatal attraction: nonself recognition and heterokaryon incompatibility in filamentous fungi, *Eukaryot. Cell* 2 (2003) 1–8.
- [2] S.J. Saupé, Molecular genetics of heterokaryon incompatibility in filamentous ascomycetes, *Microbiol. Mol. Biol. Rev.* 64 (2000) 489–502.
- [3] L. Malinina, M.L. Malakhova, A. Teplov, R.E. Brown, D.J. Patel, Structural basis for glycosphingolipid transfer specificity, *Nature* 430 (2004) 1048–1053.
- [4] L. Malinina, M.L. Malakhova, A.T. Kanack, M. Lu, R. Abagyan, R.E. Brown, D.J. Patel, The liganding of glycolipid transfer protein is controlled by glycolipid acyl structure, *PLoS Biol.* 4 (2006) e362.
- [5] T.T. Airenen, H. Kidron, Y. Nymalm, M. Nylund, G. West, P. Mattjus, T.A. Salminen, Structural evidence for adaptive ligand binding of glycolipid transfer protein, *J. Mol. Biol.* 355 (2006) 224–236.
- [6] L. Malinina, D.K. Simanshu, X. Zhai, V.R. Samyagina, R.K. Kamlekar, R. Kenoth, B. Ochoa-Lizarralde, M.L. Malakhova, J.G. Molotkovsky, D.J. Patel, R.E. Brown, Sphingolipid transfer proteins defined by the GLTP-fold, *Quart. Rev. Biophys.* 48 (2015) 281–322.
- [7] L. Malinina, D.J. Patel, R.E. Brown, How α -helical motifs form functionally diverse lipid-binding compartments, *Annu. Rev. Biochem.* 86 (2017) 609–636.
- [8] R. Kenoth, D.K. Simanshu, R.K. Kamlekar, H.M. Pike, J.G. Molotkovsky, L.M. Benson, H.R. Bergen III, F.G. Prendergast, L. Malinina, S.Y. Venyaminov, D.J. Patel, R.E. Brown, Structural determination and tryptophan fluorescence of heterokaryon incompatibility C2 protein (HET-C2), a fungal glycolipid transfer protein (GLTP), provide novel insights into glycolipid specificity and membrane interaction by the GLTP-fold, *J. Biol. Chem.* 285 (2010) 13066–13078.
- [9] R. Kenoth, R.K. Kamlekar, D.K. Simanshu, Y.-G. Gao, L. Malinina, F.G. Prendergast, J.G. Molotkovsky, D.J. Patel, S.Y. Venyaminov, R.E. Brown, Conformational folding and stability of the HET-C2 glycolipid transfer protein fold: does a molten globule-like state regulate activity? *Biochemistry* 50 (2011) 5163–5171.
- [10] P. Mattjus, B. Turcq, H.M. Pike, J.G. Molotkovsky, R.E. Brown, Glycolipid intermembrane transfer is accelerated by HET-C2, a filamentous fungus gene product involved in the cell-cell incompatibility response, *Biochemistry* 42 (2003) 535–542.
- [11] X.M. Li, M.L. Malakhova, X. Lin, H.M. Pike, T. Chung, J.G. Molotkovsky, R.E. Brown, Human glycolipid transfer protein: probing conformation using fluorescence spectroscopy, *Biochemistry* 43 (2004) 10285–10294.
- [12] R.K. Kamlekar, Y.-G. Gao, R. Kenoth, J.G. Molotkovsky, F.G. Prendergast, L. Malinina, D.J. Patel, W.S. Wessels, S.Y. Venyaminov, R.E. Brown, Human GLTP: Three distinct functions for the three tryptophans in a novel peripheral amphitropic fold, *Biophys. J.* 99 (2010) 2626–2635.
- [13] G. West, M. Nylund, J.P. Slotte, P. Mattjus, Membrane interaction and activity of the glycolipid transfer protein, *Biochim. Biophys. Acta* 1758 (2006) 1732–1742.
- [14] X. Zhai, M.L. Malakhova, H.M. Pike, L.M. Benson, H.R. Bergen III, I.P. Sugar, L. Malinina, D.J. Patel, R.E. Brown, Glycolipid acquisition by human glycolipid transfer protein dramatically alters intrinsic tryptophan fluorescence: insights into glycolipid liganding affinity, *J. Biol. Chem.* 284 (2009) 13620–13628.
- [15] H. Ohvo-Rekilä, P. Mattjus, Monitoring glycolipid transfer protein activity and membrane interaction with the surface plasmon resonance technique, *Biochim. Biophys. Acta* 1808 (2011) 47–54.
- [16] D.K. Simanshu, R.K. Kamlekar, D.S. Wijesinghe, X. Zou, X. Zhai, S.K. Mishra, J.G. Molotkovsky, L. Malinina, E.H. Hinchcliffe, C.E. Chalfant, R.E. Brown, D.J. Patel, Non-vesicular trafficking by a ceramide-1-phosphate transfer protein regulates eicosanoids, *Nature* 500 (2013) 463–468.
- [17] R.E. Brown, P. Mattjus, Glycolipid transfer proteins, *Biochim. Biophys. Acta* 1771 (2007) 746–760.
- [18] P. Mattjus, Glycolipid transfer protein and membrane interaction, *Biochim. Biophys. Acta* 1788 (2009) 267–272.
- [19] R.K. Kamlekar, D.K. Simanshu, Y.-G. Gao, R. Kenoth, H.M. Pike, F.G. Prendergast, L. Malinina, J.G. Molotkovsky, S.Y. Venyaminov, D.J. Patel, R.E. Brown, The glycolipid transfer protein (GLTP) domain of phosphoinositol 4-phosphate adaptor protein-2 (FAPP2): structure drives preference of simple neutral glycosphingolipids, *Biochim. Biophys. Acta* 2013 (1831) 417–427.
- [20] S. Neumann, M. Opacic, R.W. Wechselberger, H. Sprong, M.R. Egmond, Glycolipid transfer protein: clear structure and activity, but enigmatic function, *Adv. Enzym. Regul.* 48 (2008) 137–151.
- [21] R.E. Brown, K.L. Jarvis, K.J. Hyland, Purification and characterization of glycolipid transfer protein from bovine brain, *Biochim. Biophys. Acta* 1044 (1990) 77–83.
- [22] C.S. Rao, T. Chung, H.M. Pike, R.E. Brown, Glycolipid transfer protein interaction with bilayer vesicles: modulation by changing lipid composition, *Biophys. J.* 89 (2005) 4017–4028.
- [23] A.S. Ladokhin, S. Jayasinghe, S.H. White, How to measure and analyze tryptophan fluorescence in membranes properly, and why bother? *Anal. Biochem.* 285 (2000) 235–245.
- [24] M.K. Santra, D. Panda, Detection of an intermediate during unfolding of bacterial cell division protein FtsZ: loss of functional properties precedes the global unfolding of FtsZ, *J. Biol. Chem.* 278 (2003) 21336–21343.
- [25] R. Srivastava, A. Ratheesh, R.K. Gude, K.V.K. Rao, D. Panda, G. Subrahmanyam, Resveratrol inhibits type II phosphatidylinositol 4-kinase: a key component in pathways of phosphoinositide turnover, *Biochem. Pharmacol.* 70 (2005) 1048–1055.
- [26] C.L. Bashford, B. Chance, J.C. Smith, T. Yoshida, The behavior of oxonol dyes in phospholipid dispersions, *Biophys. J.* 25 (1979) 63–85.
- [27] I. Martin, J.M. Ruysschaert, D. Sanders, C.J. Giffard, Interaction of the lantibiotic nisin with membranes revealed by fluorescence quenching of an introduced tryptophan, *Eur. J. Biochem.* 239 (1996) 156–164.
- [28] V.R. Samyagina, A.N. Popov, A. Cabo-Bilbao, B. Ochoa-Lizarralde, F. Goni-De-Cerio, X. Zhai, J.G. Molotkovsky, D.J. Patel, R.E. Brown, L. Malinina, Enhanced selectivity for sulfate by engineered human glycolipid transfer protein, *Structure* 19 (2011) 1644–1654.
- [29] X. Zou, T. Chung, X. Lin, M.L. Malakhova, H.M. Pike, R.E. Brown, Human glycolipid transfer protein (GLTP) genes: organization, transcriptional status, and evolution, *BMC Genomics* 9 (2008) e72.
- [30] G. West, L. Viitanen, C. Alm, P. Mattjus, T.A. Salminen, J. Edqvist, Identification of a glycosphingolipid transfer protein GLTP1 in *Arabidopsis thaliana*, *FEBS J.* 275 (2008) 3421–3437.
- [31] Y. Chen, M.D. Barkley, Toward understanding tryptophan fluorescence in proteins, *Biochemistry* 37 (1998) 9976–9982.